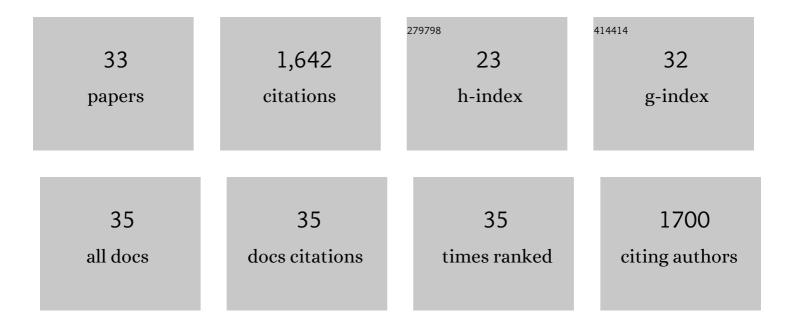
Robin J Kirkham

List of Publications by Year in descending order

Source: https://exaly.com/author-pdf/7665915/publications.pdf Version: 2024-02-01



| # | Article | IF | CITATIONS |
|----|--|-----|-----------|
| 1 | The X-ray Fluorescence Microscopy Beamline at the Australian Synchrotron. AIP Conference Proceedings, 2011, , . | 0.4 | 208 |
| 2 | Elemental X-ray imaging using the Maia detector array: The benefits and challenges of large solid-angle. Nuclear Instruments and Methods in Physics Research, Section A: Accelerators, Spectrometers, Detectors and Associated Equipment, 2010, 619, 37-43. | 1.6 | 176 |
| 3 | Maia X-ray fluorescence imaging: Capturing detail in complex natural samples. Journal of Physics: Conference Series, 2014, 499, 012002. | 0.4 | 162 |
| 4 | The New Maia Detector System: Methods For High Definition Trace Element Imaging Of Natural Material. AIP Conference Proceedings, 2010, , . | 0.4 | 89 |
| 5 | Fast X-Ray Fluorescence Microtomography of Hydrated Biological Samples. PLoS ONE, 2011, 6, e20626. | 2.5 | 89 |
| 6 | High-Definition X-ray Fluorescence Elemental Mapping of Paintings. Analytical Chemistry, 2012, 84, 3278-3286. | 6.5 | 79 |
| 7 | Maia X-ray Microprobe Detector Array System. Journal of Physics: Conference Series, 2014, 499, 012001. | 0.4 | 78 |
| 8 | The XFM beamline at the Australian Synchrotron. Journal of Synchrotron Radiation, 2020, 27, 1447-1458. | 2.4 | 75 |
| 9 | A Hidden Portrait by Edgar Degas. Scientific Reports, 2016, 6, 29594. | 3.3 | 61 |
| 10 | Reduced As components in highly oxidized environments: Evidence from full spectral XANES imaging using the Maia massively parallel detector. American Mineralogist, 2010, 95, 884-887. | 1.9 | 52 |
| 11 | Fast X-ray microfluorescence imaging with submicrometer-resolution integrating a Maia detector at beamline P06 at PETRAâ€III. Journal of Synchrotron Radiation, 2016, 23, 1550-1560. | 2.4 | 49 |
| 12 | Caenorhabditis elegans Maintains Highly Compartmentalized Cellular Distribution of Metals and Steep Concentration Gradients of Manganese. PLoS ONE, 2012, 7, e32685. | 2.5 | 47 |
| 13 | Visualizing the 17th century underpainting in Portrait of an Old Man by Rembrandt van Rijn using synchrotron-based scanning macro-XRF. Applied Physics A: Materials Science and Processing, 2013, 111, 157-164. | 2.3 | 41 |
| 14 | Correlation between Chemical and Morphological Heterogeneities in LiNi _{0.5} Mn _{1.5} O ₄ Spinel Composite Electrodes for Lithium-Ion Batteries Determined by Micro-X-ray Fluorescence Analysis. Chemistry of Materials, 2015, 27, 2525-2531. | 6.7 | 40 |
| 15 | Large detector array and real-time processing and elemental image projection of X-ray and proton microprobe fluorescence data. Nuclear Instruments & Methods in Physics Research B, 2007, 260, 1-7. | 1.4 | 34 |
| 16 | Ore Petrography Using Megapixel X-Ray Imaging: Rapid Insights into Element Distribution and Mobilization in Complex Pt and U-Ge-Cu Ores. Economic Geology, 2016, 111, 487-501. | 3.8 | 32 |
| 17 | Improved Dynamic Analysis method for quantitative PIXE and SXRF element imaging of complex materials. Nuclear Instruments & Methods in Physics Research B, 2015, 363, 42-47. | 1.4 | 31 |
| 18 | Maia Mapper: high definition XRF imaging in the lab. Journal of Instrumentation, 2018, 13, C03020-C03020. | 1.2 | 31 |

Robin J Kirkham

| # | Article | IF | CITATIONS |
|----|---|-----|-----------|
| 19 | The Maia 384 detector array in a nuclear microprobe: A platform for high definition PIXE elemental imaging. Nuclear Instruments & Methods in Physics Research B, 2010, 268, 1899-1902. | 1.4 | 29 |
| 20 | Spiral scanning X-ray fluorescence computed tomography. Optics Express, 2017, 25, 23424. | 3.4 | 28 |
| 21 | Visualising coordination chemistry: fluorescence X-ray absorption near edge structure tomography. Chemical Communications, 2016, 52, 11834-11837. | 4.1 | 26 |
| 22 | High-throughput X-ray fluorescence imaging using a massively parallel detector array, integrated scanning and real-time spectral deconvolution. Journal of Physics: Conference Series, 2009, 186, 012013. | 0.4 | 23 |
| 23 | The Maia detector array and x-ray fluorescence imaging system: locating rare precious metal phases in complex samples. Proceedings of SPIE, 2013, , . | 0.8 | 22 |
| 24 | Simultaneous X-ray fluorescence and scanning X-ray diffraction microscopy at the Australian Synchrotron XFM beamline. Journal of Synchrotron Radiation, 2016, 23, 1151-1157. | 2.4 | 19 |
| 25 | Fast XANES fluorescence imaging using a Maia detector. Journal of Synchrotron Radiation, 2018, 25, 892-898. | 2.4 | 12 |
| 26 | Next generation data acquisition systems for the CSIRO Nuclear Microprobe: Highly scaled versus customizable. Nuclear Instruments & Methods in Physics Research B, 2017, 404, 15-20. | 1.4 | 6 |
| 27 | A High-speed Detector System for X-ray Fluorescence Microprobes. , 2006, , . | | 5 |
| 28 | Validation of aGeant4model of the X-ray fluorescence microprobe at the Australian Synchrotron. Journal of Synchrotron Radiation, 2015, 22, 354-365. | 2.4 | 5 |
| 29 | A uniaxial tensile stage with tracking capabilities for micro X-ray diffraction applications. Journal of Applied Crystallography, 2011, 44, 610-617. | 4.5 | 3 |
| 30 | Preclinical studies using a prototype high-resolution PET system with Depth of Interaction. , 2011, , . | | 3 |
| 31 | SiPM based detector module and digital data acquisition system for PET: Initial results. , 2009, , . | | 1 |
| 32 | High-definition mapping of trace metal elements in the hippocampus in a model of closed-head traumatic brain injury. Injury, 2010, 41, S30-S31. | 1.7 | 1 |
| 33 | Maia Mapper: High Definition XRF Imaging of Geological Samples at Intermediate Spatial Scales. Microscopy and Microanalysis, 2018, 24, 110-111. | 0.4 | 1 |